1994-08-01

Single mRNAs visualized by ultrastructural in situ hybridization are principally localized at actin filament intersections in fibroblasts

Gary J. Bassell
University of Massachusetts Medical School

Et al.

Single mRNAs Visualized by Ultrastructural In Situ Hybridization Are Principally Localized at Actin Filament Intersections in Fibroblasts

Gary J. Bassell, Christine M. Powers, Krishan L. Taneja, and Robert H. Singer

Department of Cell Biology, University of Massachusetts Medical Center, Worcester, Massachusetts 01655-0106

Abstract. Considerable evidence indicates that mRNA associates with structural filaments in the cell (cytoskeleton). This relationship would be an important mechanism to effect mRNA sorting since specific mRNAs could be sequestered at sites within the cell. In addition, it can provide a mechanism for spatial regulation of mRNA expression. However, the precise structural interactions between mRNA and the cytoskeleton have yet to be defined. An objective of this work was to visualize "individual" poly(A) mRNA molecules in situ by electron microscopy to identify their relationship to individual filaments. Poly(A) RNA and filaments were identified simultaneously using antibodies to detect hybridized probe and filaments or actin-binding proteins. In human fibroblasts, most of the poly(A) mRNA (72%) was localized within 5 nm of orthogonal networks of F-actin filaments. Poly(A) mRNA also colocalized with vimentin filaments (29%) and microtubules (<10%). The sites of mRNA localization were predominantly at filament intersections. The majority of poly(A) mRNA and polysomes colocalized with the actin crosslinking proteins, filamin, and α-actinin, and the elongation factor, EF-1α (actin-binding protein; ABP-50). Evidence that intersections contained single mRNA molecules was provided by using a labeled oligo dT probe to prime the synthesis of cDNA in situ using reverse transcriptase. Both the poly(A) and *cis* sequences of the same mRNA molecule could then be visualized independently. We propose that the cytoskeletal intersection is a mRNA receptor and serves as a "microdomain" where mRNA is attached and functionally expressed.

THERE is now considerable evidence that indicates mRNA is associated with the cytoskeleton (reviewed in Nielson et al., 1983; Hesketh and Pryme, 1991). Extraction of the cell by nonionic detergent leaves the majority of mRNA and polyribosomes contained within an insoluble cytoskeletal fraction, whereas monomeric ribosomes are contained in the soluble fraction (Lenk et al., 1977; Jeffrey, 1982; Zambetti et al., 1985; Fulton et al., 1980; Ornelles et al., 1986). The mRNAs of certain viruses are translated only when associated with the cytoskeleton; therefore, this interaction may be obligatory for protein synthesis (Lenk and Penman, 1979; Cervera et al., 1981; van Venrooij et al., 1981; Ben-Ze'ev et al., 1981; Bonneau et al., 1985). The association of mRNAs to the cytoskeleton also functions to localize mRNAs to specific cytoplasmic compartments (Singer, 1992). This association is of interest because it provides a mechanism for the anchoring of specific mRNAs which become localized and therefore can provide site(s) where translation of specific proteins occurs intracellularly (Sundell and Singer 1991; Singer, 1992).

Address all correspondence to G. J. Bassell, Center for Neurologic Disease, Brigham and Women's Hospital, 221 Longwood Avenue, Boston, MA 02115.

The mechanism of the association of mRNA to the cytoskeleton remains unclear. Messenger RNA has been shown to be released from the cytoskeleton in several cell types using the actin depolymerizing drug cytochalasin (Lenk et al., 1977; Zambetti et al., 1985; Ornelles et al., 1986; Taneja et al., 1992) which also decreases protein synthesis (Ornelles et al., 1986). Disruption of the filament system, however, prevents the direct analysis of the mechanism by which mRNA was associated with the actin cytoskeleton and how this interaction may influence translation. Poly(A) mRNA has been shown to codistribute with actin filaments using double label immunofluorescence combined with digital image analysis (Taneja et al., 1992). However, it has not been possible to demonstrate a direct association of poly(A) with microfilaments with the level of resolution provided by light microscopy (0.2 μm). Therefore, a direct, high resolution approach to study the distribution of mRNA with the fibroblast cytoskeleton was undertaken which allowed visualization of individual molecules and their precise sites of localization (Bassell, 1993). By using ultrastructural detection of oligo dT probes hybridized in situ, the nanometer resolution proximated poly(A) RNA molecules to specific individual filament structures. Since at least 90% of eukaryotic

mRNAs are polyadenylated (Sheiness and Darnell, 1973; Brawerman, 1981), these observations could be generalized to most mRNAs. This analysis demonstrated that poly(A) mRNA was not uniformly distributed along filaments, but localized at intersections. Poly(A) mRNA was principally localized within the actin cytoskeleton compartment, specifically at vertices, and near the actin-binding proteins, EF1α, filamin, and α-actinin. Poly(A) RNA was also colocalized with intermediate filaments to a significant amount and to a lesser amount to microtubules. Methodology developed to resolve single mRNA molecules suggested that most of these cytoskeletal attachment sites in fact contained only one mRNA. This site possibly represents the functional compartment where specific mRNAs become immobilized within a translational complex.

Materials and Methods

Technology Development

Characterization of the specific cytoskeletal proteins localized in proximity to mRNA (with 10 nm) was possible by improving double labeling methods. The identification of the cytoskeletal filament system(s) colocalized with poly(A) required several modifications to the existing methodology. Monoclonal antibody labeling of filaments was sparse following a 3-h hybridization in 50% formamide, and did not uniformly decorate microfilaments or intermediate filaments (Singer et al., 1989). An objective of this work was to improve the labeling such that mRNA-filament colocalization could be directly visualized.

Optimization required evaluation of the effects of various fixation and hybridization conditions on the characteristic filament staining patterns seen with cytoskeletal antibodies and assessed by using silver enhancement at the light microscope level. An immediate advantage of hybridization to poly(A) with oligo-dT probes was that due to the lower melting temperature of A-T hybrids, significantly less stringent hybridization conditions were required than with actin mRNA hybrids. This allowed minimal use of formamide, a strong denaturant. In addition, the hybridization time was reduced from 3 h to 30 min and resulted in less disruption of antigenicity and a consequent increase in the density of antibody labeling along filaments. Alternative fixation methods were also evaluated. 4% glutaraldehyde resulted in strong hybridization signal, and superior ultrastructural preservation, although antibody labeling of CSK proteins was only fair. The best compromise in morphology and labeling was obtained with fixations in 2% formaldehyde/0.2% glutaraldehyde (see Fig. 5). These combined optimizations were sufficient to obtain characteristic light microscopy staining patterns for microtubules, intermediate filaments and microfilaments (see Fig. 1) and permitted their ultrastructural identification by electron microscopy.

Cell Culture

Human diploid fibroblasts (provided by Edward Fey, University of Massachusetts Medical School) were used for most of this work. Chick embryo fibroblasts and the rabbit RK13 epithelium cell line (American Type Culture Collection, Rockville, MD) were used for supportive data. Cells were cultured by standard techniques and plated in Falcon six-well tissue culture plates at a density of 2×10^5/well. Tissue culture plates contained sterile coverslips (thin section procedure) or carbon and formvar (0.5% in dichloroethane) coated gold EM grids on 22-mm circular coverslips (whole-mount procedure). The purity of the gold grid was essential for cell viability, and 100% gold grids were obtained from Ladd Inc. (London 200 mesh, 3 mm; Burlington, VT). Grid assemblies were made by floating a formvar film onto glass coverslips supporting six gold grids. After drying, the film was coated with carbon using a Denton Evaporator (Denton Vacuum Inc., Cherry Hill, NJ). Grid assemblies were sterilized by gamma irradiation from a cesium-137 source.

For whole-mount analysis, cells were Triton extracted and/or fixed 1–2 d after plating. The Triton-extraction (CSK) buffer (Lenk et al., 1977) contained: 0.3 M sucrose, 0.1 M NaCl, 10 mM Pipes, pH 6.9, 3 mM $MgCl_2$, 10 μM leupeptin (Sigma Chemical Co., St. Louis, MO), 2 mM dilution Vanadate–ribonucleotide complex (4 mM adenosine, 0.2 M $VaSO_4$). To disorganize actin filaments, cells were treated with cytochalasin D at 0.5 μg/ml for 30 min before Triton extraction. Cells were briefly washed with CSK buffer, and then extracted for 60–90 s at 4°C in CSK buffer containing 0.5% Triton X-100, followed by a brief wash in the first buffer and then fixed in 2% formaldehyde/0.2% glutaraldehyde or 4% glutaraldehyde (PBS containing 5 mM $MgCl_2$). Cells not extracted with Triton X-100 were first washed in Hanks' balanced salt solution and then fixed in 4% formaldehyde (PBS, 5 mM $MgCl_2$). All fixations were for 15 min at room temperature. Cells were processed for in situ hybridization and immunocytochemistry directly following fixation.

Probe Preparation

Synthetic (Applied Biosystems Synthesizer 396; Applied Biosystems, Foster City, CA) oligo-dT (55 nt) and oligo-dA (55 nt) were 3' end labeled with biotin-16-dUTP (Boehringer Mannheim Biochemicals, Indianapolis, IN) using terminal deoxynucleotide transferase (25 pM oligo, 25 mM biotin dUTP, 140 mM potassium cacodylate, 30 mM Tris-HCl, pH 7.6, 1 mM $CoCl_2$, 0.1 mM DTT, and 100 U of terminal transferase) at 37°C for 1 h. Alternatively, synthetic oligo dT (or oligo dA) was 5' end labeled using biotin succinamide ester to react an amino group with a single C6 amino-modified thymidine at the 5' end (Glen Research, Sterling, VA). Probes were purified using a 20 ml G-50 column, and aliquots of the collected fractions were blotted onto nitrocellulose and detected using a streptavidin–alkaline phosphatase conjugate (Boehringer Mannheim Biochemicals). Positive fractions were lyophilized, resuspended, combined, and the optical density measured. The size of the biotinated terminal transferase tails were approximately 10-bases long as determined by polyacrylamide gel electrophoresis.

Hybridization

Cells were washed in PBS (5 mM $MgCl_2$) and then equilibrated in 15% formamide (Sigma Chemical Co.) 2× SSC and 10 mM sodium phosphate pH 7.0, at room temperature for 10 min. 5 to 20 ng of probe was dried down with *Escherichia coli* tRNA (10 μg) and sonicated salmon sperm DNA (10 μg), and then suspended in 10 μl of 30% formamide containing 20 mM sodium phosphate, pH 7.0. Probes were mixed with 10 μl of hybridization buffer (20% dextran sulfate, 4× SSC, 0.4% BSA, 20 mM sodium phosphate, pH 7.0). Coverslips were placed cell side down on parafilm containing 20 μl probe mixture and hybridized for 0.5–3 h at 37°C. After hybridization, coverslips were washed for 20 min in 15% formamide 2× SSC at 37°C, and three 10-min washes in 1× SSC on a rotary shaker at room temperature.

Immunocytochemistry

Detection of biotinated probes was accomplished by a two-step immunogold procedure using rabbit antibiotin primary antibodies (Enzo Biochem. Corp., New York) and colloidal gold (1.4 or 10 nm) labeled goat anti-rabbit secondary antibodies or protein A–colloidal gold (10 nm) (Amersham Corp., Arlington Heights, IL). Detection of digoxigenin-labeled nucleotides (Boehringer Mannheim Biochemicals) was accomplished using sheep polyclonal antibodies to digoxigenin directly conjugated to gold particles (5 nm; Biocell Laboratories, Ted Pella Inc., Redding, CA). Coverslips were pretreated with 8% BSA, RNAse free (Boehringer Mannheim Biochemicals) in TBS (150 mM, NaCl, 50 mM Tris, pH 7.4) for 10 min. Primary antibodies were diluted 1:100 in 1% BSA, 0.1% Triton X-100, TBS, pH 7.4 (BTTBS), and incubated at 37°C for 1 h. Coverslips were washed three times in BTTBS for 10-min each on a rotary shaker at room temperature. Coverslips were incubated with colloidal gold–labeled antibodies (1:25 dilution in BTTBS) for 2 h at 37°C and washed as above.

For silver enhancement of colloidal gold, samples were washed thoroughly in double-distilled deionized water and placed into dry multiwell plates (cell side facing up). Approximately 300 μl of silver enhancement reaction solution (Amersham Corp.) was added to each sample, and the enhancement was observed in progress using a 40× water immersion objective. Visualization of brown-colored cellular staining indicated a positive signal and the reaction was terminated. The time taken in the silver enhancement reaction for a strong visual signal to be observed varied and was a function of the size of the gold particle and extraction/fixation conditions. The methodological development of silver enhancement for correlative light and electron microscopic in situ hybridization (ISH)[1] has been reported (Bassell and Singer, 1993).

Detection of cytoskeletal proteins was accomplished in analogous fash-

1. *Abbreviations used in this paper*: ISH, in situ hybridization; IST, in situ transcription.

ion to biotinated probes. Several monoclonal antibodies were screened by light and electron microscopy using silver enhancement of 1.4-nm gold-labeled goat anti-mouse secondary antibodies (Amersham Corp.). The objective was to obtain monoclonals which reacted after glutaraldehyde fixation (2% formaldehyde/0.2% glutaraldehyde) in order to preserve the ultrastructural morphology of polysomes and cytoskeletal filaments. Also, the monoclonals had to exhibit strong labeling followed a hybridization in 15% formamide, 2× SSC for 30 min. The following antibodies were selected for this study: anti-actin (East Acres Biologicals, Southbridge, MA; Boehringer-Mannheim Biochemicals), anti-vimentin (Boehringer Mannheim Biochemicals; Amersham Corp.), anti-tubulin (Amersham Corp.), anti-filamin (Sigma Chemical Co.; Amersham Corp.), and anti-α-actinin (Sigma Chemical Co.). Rabbit polyclonal antibodies to Artemia EF1α was kindly provided by Wim Moller (Rijks University, Leiden, The Netherlands) (Sanders et al., 1994). Antibody specificity was confirmed on Western blots (data not shown). For double labeling of cytoskeletal proteins and poly(A) mRNA, rabbit antibiotin antibodies to detect the probe were incubated with the above monoclonals. Similarly, goat anti-rabbit (10-nm gold) antibodies were incubated with goat anti-mouse (5-nm gold) antibodies in the secondary incubation. To detect poly(A) and EF1α, digoxigenin-labeled oligo-dT was detected with directly conjugated sheep antibodies (10 nm) and EF1α was detected with goat anti-rabbit antibodies (5 nm).

In Situ Transcription

After posthybridization washes, samples were incubated at 37°C for 60 min with the following: reverse transcriptase (avian myoblastosis virus; Boehringer Mannheim Biochemicals, 600 U/ml); ribonuclease inhibitor (RNAsin, 0.12 U/μl; Boehringer Biochemicals); unlabeled nucleotides (TTP, dCTP, cATP, dGTP at 250 μM); biotin-16-dUTP or digoxigenin-11-dUTP (50 μM; Boehringer Mannheim Biochemicals); in a 50 mM Tris-HCl buffer (pH 8.3) with 6 mM $MgCl_2$, 40 mM KCl, 7.5 mM dithiothreitol. Samples were twice washed in 15 or 50% formamide in 2× SSC for 30 min at 37°C.

Controls

For in situ hybridization, control biotinated oligo-dA probes were hybridized in parallel to oligo-dT in all experiments. Both oligo-dT and oligo-dA hybridizations were evaluated ultrastructurally. 10-nm colloidal gold-labeled antibody samples which were evaluated at the electron microscope, quantitation of signal-to-noise ratios was obtained by counting gold particles per area in oligo-dT and oligo-dA samples (Fig. 3). Also, parallel oligo-dT and oligo-dA samples were silver enhanced for light microscopic signal-to-noise evaluation (see Fig. 1). The use of excess unlabeled oligo-dT hybridized as a competitor to biotinated oligo-dT served as an alternative control, and provided identical background levels compared to biotinated oligo-dA probes.

In situ transcription using unlabeled oligo-dT as a primer was controlled by reactions without primer, or using oligo-dA, or heat inactivated enzyme. Signal-to-noise ratios of all reactions were evaluated at the light microscopic level using silver enhancement detection followed by ultrastructural analysis.

Electron Microscopy

For analysis by thin sectioning, coverslips were postfixed in 2% osmium tetroxide in PBS for 30 min. After rinsing in distilled H_2O, samples were dehydrated to absolute ethanol through a series of graded ethanol dilutions. After treatment with a 1:1 mixture of propylene oxide and Poly/bed 812 (Polysciences, Inc., Warrington, PA) for 30–60 min at room temperature, samples were placed into 100% Poly/bed 812 for 1 h at room temperature. Beem capsules were filled with fresh 100% Poly/bed 812 and quickly inverted onto the surface of the coverslips and polymerized for 48 h at 60°C. To remove the Beem capsules from the coverslip, samples were immersed in liquid nitrogen for a few seconds, and gently tapped to remove the Beem capsule. Thin sections (60–80 nm) were cut using an LKB ultramicrotome and diamond knife, and were stained with uranyl acetate (1.5 in 50% ethanol), and Reynold's lead citrate for 3 and 5 min, respectively.

For analysis by whole mounts, grids were teased from coverslips, and dehydrated. Samples were dried through the critical point of CO_2 using a Samdri PVT-3. All samples were evaluated with a Philips 400 transmission electron microscope.

Postembedment Methodology

Procedures for Lowicryl embedding described previously (Bendayan, 1983; Altman et al., 1984) were adapted for use with postembedment in situ hybridization. Pectoral muscle from 16-d embryonic chickens was fixed immediately after dissection by immersion in 2% formaldehyde/0.1% glutaraldehyde (PBS, 5 mM $MgCl_2$) for 1 h at 4°C. During fixation, the muscle was cut into 1–2-mm cubes for further handling. After washing in PBS, the tissue blocks were washed in 0.5 M NH_4Cl (PBS) for 90 min at 4°C to quench the free aldehyde groups (Biggiogera et al., 1989). Following additional PBS washes, the tissue was dehydrated through increasing concentrations of dimethylformamide before infiltration with Lowicryl K4M (Polysciences, Inc.).

Blocks were placed in Lowicryl filled Beem capsules suspended between two 15-W UV light sources, 10 cm from each source. Foil reflectors were positioned around the capsules to reflect the light from all directions and a fan was used to disperse the heat while polymerization took place for 45 min at room temperature.

Thin sections (60–80 nm) were collected on pure gold grids. Hybridization conditions were similar to those described for coverslips. For biotin-labeled probe and antibody incubations, grids were floated on 20-μl drops of the appropriate solution in a humidified chamber with a dust cover for protection. Washes were accomplished by gently dipping each grid into a beaker of the buffer 10–12 times for each. After a final wash with a gentle stream of distilled water from a wash bottle, grids were stained with saturated uranyl acetate (45 s) and Reynold's lead citrate (10 s) before evaluation with a Philips 400 transmission electron microscope.

Results

Intracellular Poly(A) mRNA Distribution Using Silver-enhanced Gold Viewed by Light Microscopy

The intracellular distribution of poly(A) mRNA in both Triton-extracted (Fig. 1 *A*) and unextracted cells (Fig. 1 *C*) was visualized using hybridization of biotinated oligo-dT probes, detected by silver enhancement of an anti-rabbit antibody conjugated to colloidal gold. In many nuclei of Triton-extracted cells, a patchy distribution of poly(A) mRNA was observed (Fig. 1 *A*) as described previously (Carter et al., 1991). Nuclear hybridization could not be easily detected with gold-labeled antibodies in unextracted cells (Fig. 1 *C*), and visualization required use of low molecular weight reagents, i.e., streptavidin (data not shown). Strong cytoplasmic signal was seen in >95% of the Triton-extracted or -unextracted cell populations. Greater than 90% of mRNA in these cells was retained following a 1-min Triton extraction (Taneja et al., 1992). Very low background levels were detected using an oligo-dA probe (Fig. 1 *B*).

Cytoplasmic poly(A) mRNA was not uniformly distributed but was patchy and most abundant perinuclearly where the cytoplasm was thickest. The periphery, where the cell is thinnest, exhibited comparatively less staining, and the leading edge or lamellipodia was not labeled. The distribution of poly(A) mRNA did not exhibit an obvious fibrillar appearance, which would visually reflect the distribution of microfilaments (e.g., stress fibers) detected by antibody to actin (Fig. 1 *D*). These patterns were observed in both extracted and unextracted cells (Fig. 1, *A* and *C*). The use of silver enhancement of 1.4-nm gold-labeled antibodies allowed correlation of light and electron microscopic observations in extracted and unextracted cells; antibodies complexed to larger gold particles do not easily penetrate the cytoplasm of unextracted cells (Bassell et al., 1993). Cytochalasin D treatment resulted in a major alteration in the distribution and retention of poly(A) mRNA on the cytoskeleton (Fig. 1 *E*), perinuclear and nuclear poly(A) mRNA were still evident. Stress fibers were no longer observed following cytochalasin D

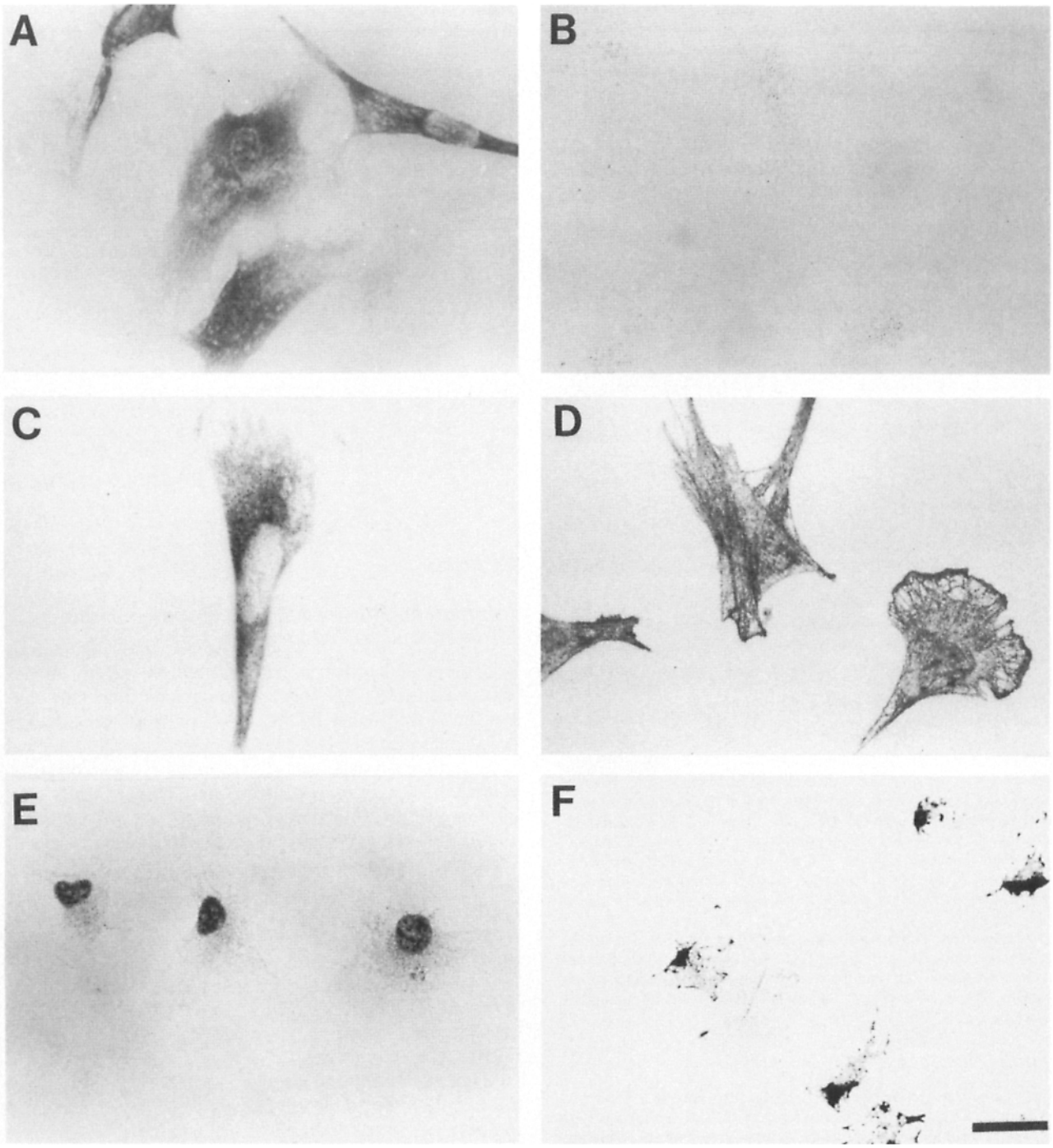

Figure 1. Detection of poly(A) mRNA or actin filaments using silver-enhanced 1-nm gold. (*A*) Oligo-dT-biotin hybridization to Triton-extracted, paraformaldehyde (2%), and glutaraldehyde (0.2%) fixed fibroblasts. Patchy cytoplasmic distribution and some nuclear focal concentrations of poly(A) are detected. (*B*) Control hybridization with oligo-dA-biotin showed no staining. (*C*) Oligo-dT-biotin hybridization to a paraformaldehyde fixed fibroblast not extracted before fixation; (*D*) Anti-actin staining in Triton-extracted fibroblasts. Actin stress fibers, lamellipodia and microspikes are evident. (*F*) Hybridization to poly(A) mRNA following cytochalasin D treatment and Triton extraction. The majority of mRNA is released from the cytoskeleton. Nuclear and perinuclear hybridization is still evident. (*F*) Anti-actin labeling following cytochalasin D treatment and Triton extraction. Actin protein is released from cytoskeleton, and disorganized actin filaments are localized in aggregates. Bar, 25 μm.

treatment, and actin labeling was localized in cytoplasmic aggregates (Fig. 1 *F*). These data confirm an involvement of actin in the distribution of poly(A) mRNA (Taneja et al., 1992). The detection of enhanced colloidal gold antibodies at the light microscope level could yield images with resolution equivalent to fluorescence. However, an additional advantage is that the same samples could be examined at the ultrastructural level after viewing by light microscopy.

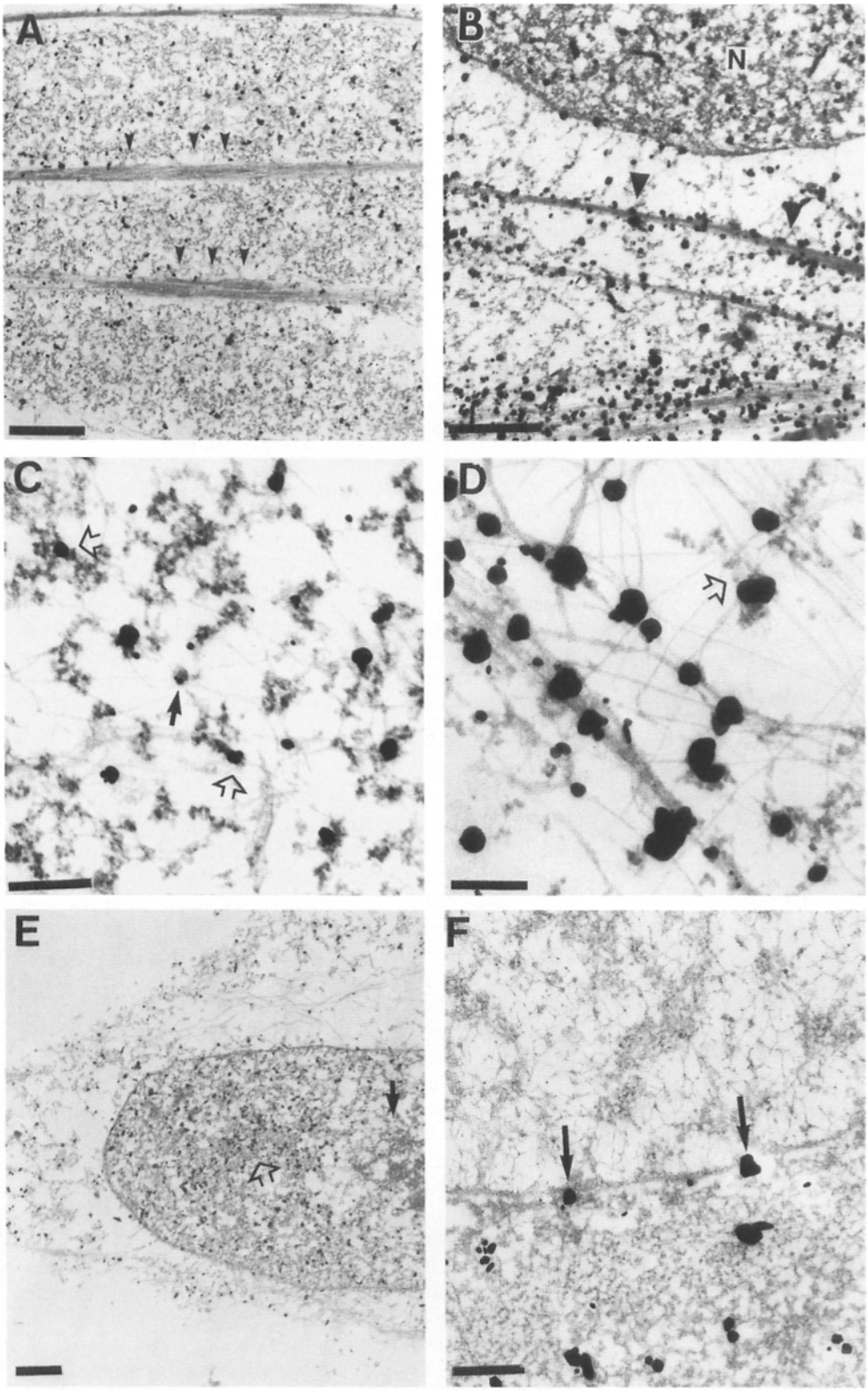

Figure 2. Ultrastructural distribution of poly(A) mRNA, polysomes, and actin protein using thin section EM. Detection of silver enhanced 1-nm colloidal gold labeled secondary antibodies, followed by embedment and thin sectioning. (*A*) Oligo-dT-biotin hybridization to a Triton-extracted fibroblast. Poly(A) is not localized within stress fibers (*arrowheads*). (*B*) Localization of actin protein to stress fibers (*arrowheads*), and diffuse networks throughout the cytoplasm in a Triton-extracted fibroblast. Nuclear labeling is also detected (*N*, nucleus). (*C*) Oligo-dT-biotin hybridization to a Triton-extracted fibroblast. Poly(A) mRNA was observed to colocalize with morphologically identifiable polysomes (*open arrows*). Poly(A) mRNA appears concentrated near regions of filament intersection (*arrow*). (*D*) Association of polysomes with filaments labelled with anti-actin antibodies (*open arrow*). (*E*) Hybridization to nuclear poly(A) RNA in a Triton-extracted cell was clustered around interchromatin granules (*open arrow*). Comparatively less hybridization was seen within nucleoli (*arrow*). (*F*) Oligo-dT-biotin hybridization to a fibroblast which was not extracted with Triton before fixation. A clustery distribution of poly(A) mRNA was observed throughout the perinuclear cytoplasm. Cytoskeletal filaments are not, however, visible in unextracted cells. Poly(A) mRNA was also detected in association with nuclear pores (*arrows*). Bars: (*A, B, E*) 1 μm; and (*C, D, F*) 250 nm.

Ultrastructural Distribution of Poly(A) mRNA, Polysomes, and Filaments

Cells were then processed for thin section electron microscopy. At the ultrastructural level, the silver particles were visible at low magnification, and provided a continuum between optical and ultrastructural observations. Although poly(A) was distributed throughout the cytoplasm, it was concentrated in areas indicated by aggregates of silver particles, surrounded by unlabeled regions. Silver particles were often close together or fused, suggesting the presence of aggregates of mRNA molecules (Fig. 2, *A*, *C*, *E*, and *F*). The clustered distribution was observed in both Triton-extracted and -unextracted cells. In unextracted cells which were Epon

embedded, cytoskeletal filaments and polysomes were not visualized (Fig. 2 *F*). In Triton-extracted cells, however, the cytoskeleton and polysomes were easily visualized because the cytosol was removed and therefore their spatial relationship to mRNA could be analyzed (Fig. 2, *A*, *C*, and *E*). Poly(A) was seen colocalized with cytoskeletal filaments and morphologically identifiable polyribosomes (84% of the poly[A] signal colocalized with ribosomes, $n = 175$ silver particles; Fig. 2 *C*). Polysomes were identified by their characteristic morphology, often present in circular or coiled conformations. Poly(A) was not uniformly distributed along filaments, but was concentrated at intersections when viewed by the electron microscope (Fig. 2 *C*, *arrow*). Stress fibers did not contain large amounts of poly(A) mRNA, but hybridization was detected at their surfaces (Fig. 2 *A*). The majority of poly(A) was localized to a diffuse network of thin, branched filaments which were not tightly bundled.

Unlike the distribution of oligo dT label, detection of actin protein using silver enhancement demonstrated strong labeling of microfilament bundles (stress fibers), in addition to the networks of microfilaments (Fig. 2 *B*). Polysomes were localized to microfilaments identified using actin antibodies (Fig. 2 *D*). Similar to the poly(A), polysomes were not distributed linearly along microfilaments, but tended to cluster at specific points (Fig. 2 *D*, *arrow*).

Detection of Nuclear Poly(A)

Poly(A) could also be detected by high resolution in situ hybridization in the nucleus. Poly(A) appeared associated with electron-dense material (Fig. 2 *E*) which may coincide with the interchromatin granules (see also observations by Visa et al. 1993). Of interest was the poly(A) mRNA near nuclear pores (Fig. 2 *F*). In Triton-extracted cells, nuclear actin (or an immunologically related protein) was also detected with a monoclonal antibody (Fig. 2 *B*). The presence of actin within the Triton-insoluble nuclear matrix has been described (Nakayasu and Ueda, 1986; Nakayasu et al., 1985*a*). A role of nuclear actin in RNA metabolism has also been suggested (Scheer et al., 1984; Nakayasu et al., 1985*b*).

Localization of Poly(A) to Filament Intersections

An evaluation of the spatial distribution of poly(A) mRNA within thin sections was limited by the lack of three-dimensional information and diminished contrast due to the embedment (Nickerson and Penman, 1991). Thin sections (60–80 nm) prevent sufficient depth of view; therefore, filaments appear fragmented, producing strictly a two-dimensional viewpoint of the spatial relationship between poly(A) mRNA and the cytoskeleton. Triton-extraction removes ~70% of total cellular protein providing sufficient contrast to examine the cytoskeleton using whole-mount electron microscopy (Lenk et al., 1977; Pudney and Singer, 1979).

Consistent with the results obtained from thin sections (Fig. 2 *C*), examination of the poly(A) mRNA signal in whole mounts at high magnification revealed a clustered appearance which suggested that poly(A) mRNA was not uniformly distributed along cytoskeletal filaments. Although the large size of the silver particle (100–200 nm) obscured the exact sites of mRNA localization it appeared that poly(A) resided where filaments intersected. To further evaluate this observation, the localization of poly(A) to intersections was visualized and quantitated using colloidal gold–labeled antibodies (10-nm gold particles) which were not silver enhanced. The signal was evident as individual gold particles and dense clusters of particles (Figs. 3 and 4). A signal to noise ratio of 7.6:1 was obtained for single gold particles (oligo-dT/oligo-dA) and increased to 17.8:1 when three or more particles were present within a cluster (Fig. 3). The high signal to noise indicated that bona fide detection of poly(A) RNA had occurred (95% confidence). Most of the signal was detected as single particles (67%), only rarely were more than five particles in a cluster observed (4.2%). Clusters of gold particles could be attributed to the binding of multiple primary antibiotin antibodies to a single probe molecule, and binding of multiple secondary antibodies to a single primary antibody (see below).

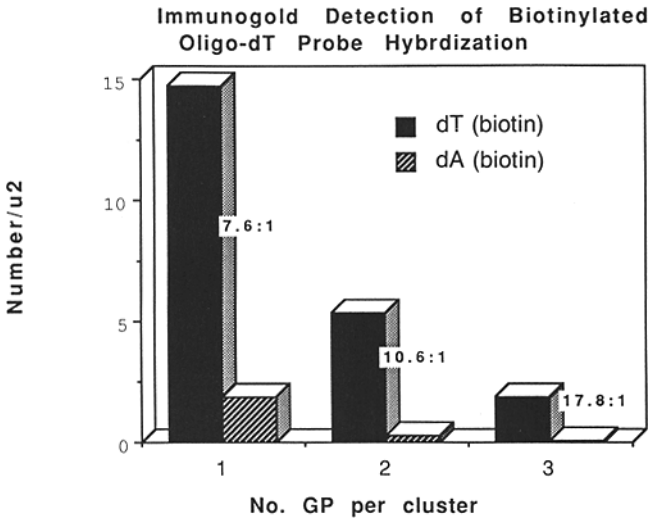

Figure 3. Ultrastructural quantitation of in situ hybridization using immunogold. The signal to noise ratio between oligo dT and oligo dA probes was determined using detection of single and multiple gold clusters. Analysis of 50 electron micrographs at 28,000X from perinuclear, central and peripheral regions from ten cells in oligo-dT (biotin) samples and six cells in control oligo-dA (biotin) samples. Data from three independent hybridizations to Triton-extracted, glutaraldehyde (4%) fixed fibroblasts. Hybridization signal was detected as single gold particles and clusters of gold particles. Signal-to-noise ratios for single gold particles and each size gold particle cluster are indicated.

The majority of gold particles (>76%) (signal which could be scored for localization to filaments or vertices) were localized to cytoskeletal intersections and not uniformly distributed along individual filaments (Fig. 4, *A–C*). The labeled intersections exhibited complex branching patterns and were composed of between two to five filaments. To verify that the gold particles were directly localized to intersections, hybridization was visualized using stereo pairs (data not shown) and thin sectioning (Fig. 4 *C*). Occasionally hybridization also localized to sites along single filaments (Fig. 4 *D*).

Colocalization of Poly(A) with Filament Systems and Actin-binding Proteins

To confirm directly the identity of filament systems with which poly(A) was localized, poly(A) mRNA was visualized with 10-nm gold in conjunction with antibodies to cytoskele-

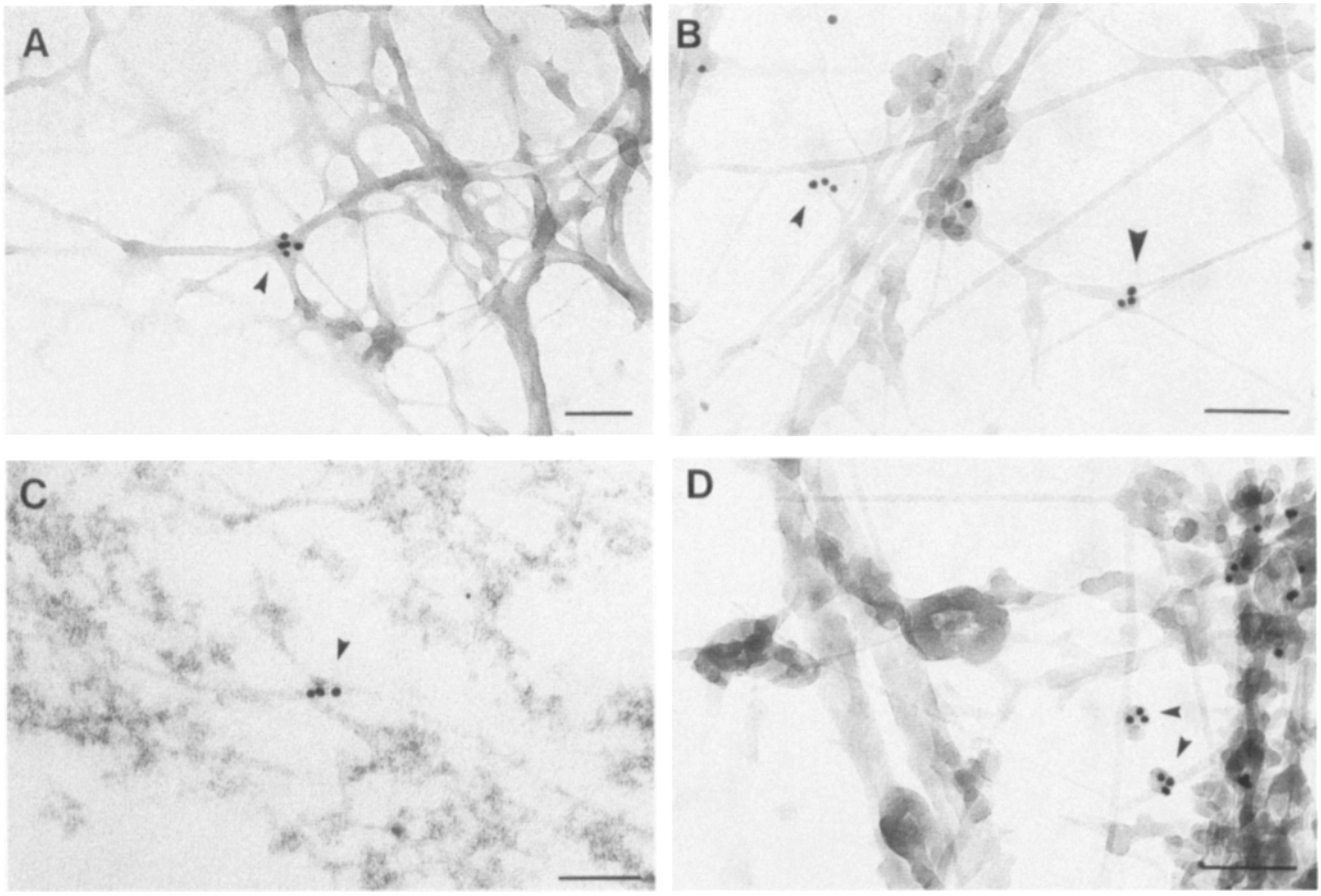

Figure 4. Localization of poly(A) mRNA to cytoskeletal filament intersections. Detection of oligo-dT-biotin by immunogold in Triton-extracted, glutaraldehyde (4%) fixed fibroblasts. (*A*) Highly branched vertex (*arrow*) with associated poly(A) mRNA seen after critical point drying. Majority of scored hybridization signal (76%) was localized to vertices (within 10 nm). (*B*) Poly(A) mRNA associated with an intersection of two filaments (*large arrow*), and along an individual filament, but within 10 nm of intersection (*small arrow*). Critical point dried sample. (*C*) Thin section of an intersection containing poly(A) mRNA. (*D*) Poly(A) mRNA localized to points along individual filaments (*arrows*). Critical point dried sample. Bar, 100 nm.

tal proteins detected with 5-nm gold. This double label approach was used in whole mounts to quantitate the colocalization of poly(A) mRNA in pairwise combination with actin, tubulin, vimentin, and three actin binding proteins. Poly(A) mRNA molecules scored as localized to a particular filament were required to meet two criteria: (*a*) the 10-nm particle(s) was within 5 nm of one in a series of 5-nm particles; and (*b*) both sizes of colloidal gold visually appeared to be localized to the same filament. These strict criteria therefore limited the number of poly(A) mRNA molecules that could be evaluated in the whole-mount preparation. In addition, in thick cytoskeletal regions, it was frequently not possible to distinguish whether a 10-nm particle was localized to a labeled filament or an immediately adjacent unlabeled filament. Therefore, only poly(A) mRNA which could be scored unequivocally for their proximity to a labeled protein or identifiable filament were included in the analysis. Despite these restrictions, the whole mounts yielded substantially more poly(A) signal than thin sections of the sample.

The result of this analysis is summarized in Table I and Fig. 5 (*A–C*) and is compiled from three independent experiments. The majority of poly(A) mRNA was observed to be localized to the actin cytoskeleton in agreement with previous work using fluorescent detection of poly(A) and quantitative imaging microscopy (Taneja et al., 1992). However, the use of colloidal gold for detection of poly(A) and filaments allowed much higher resolution and provided highly accurate analyses, since individual molecules of poly(A) were counted and individual filaments were visualized. 72% of the poly(A) detected was found to be localized within 5 nm of labeled microfilaments. This result was consistent with the thin sections analysis (see Fig. 2 *D*), where polysomal dense regions were primarily composed of actin filaments. The density of gold particles representing poly(A) signal along microfilaments was significantly lower and less uniform than signal obtained by labeling with a monoclonal antibody to actin. Poly(A) appeared concentrated at microfilament intersections (Fig. 5 *A*), whereas antiactin binding labeled the length of the filament.

Poly(A) was also observed to colocalize with vimentin filaments (29%). These results were obtained using two different monoclonal antibodies and two different cell types. In regions of the cell where the intermediate filaments predominated, the poly(A) mRNA–vimentin colocalization was most clearly evident (Fig. 5 *B*). Analogous to the

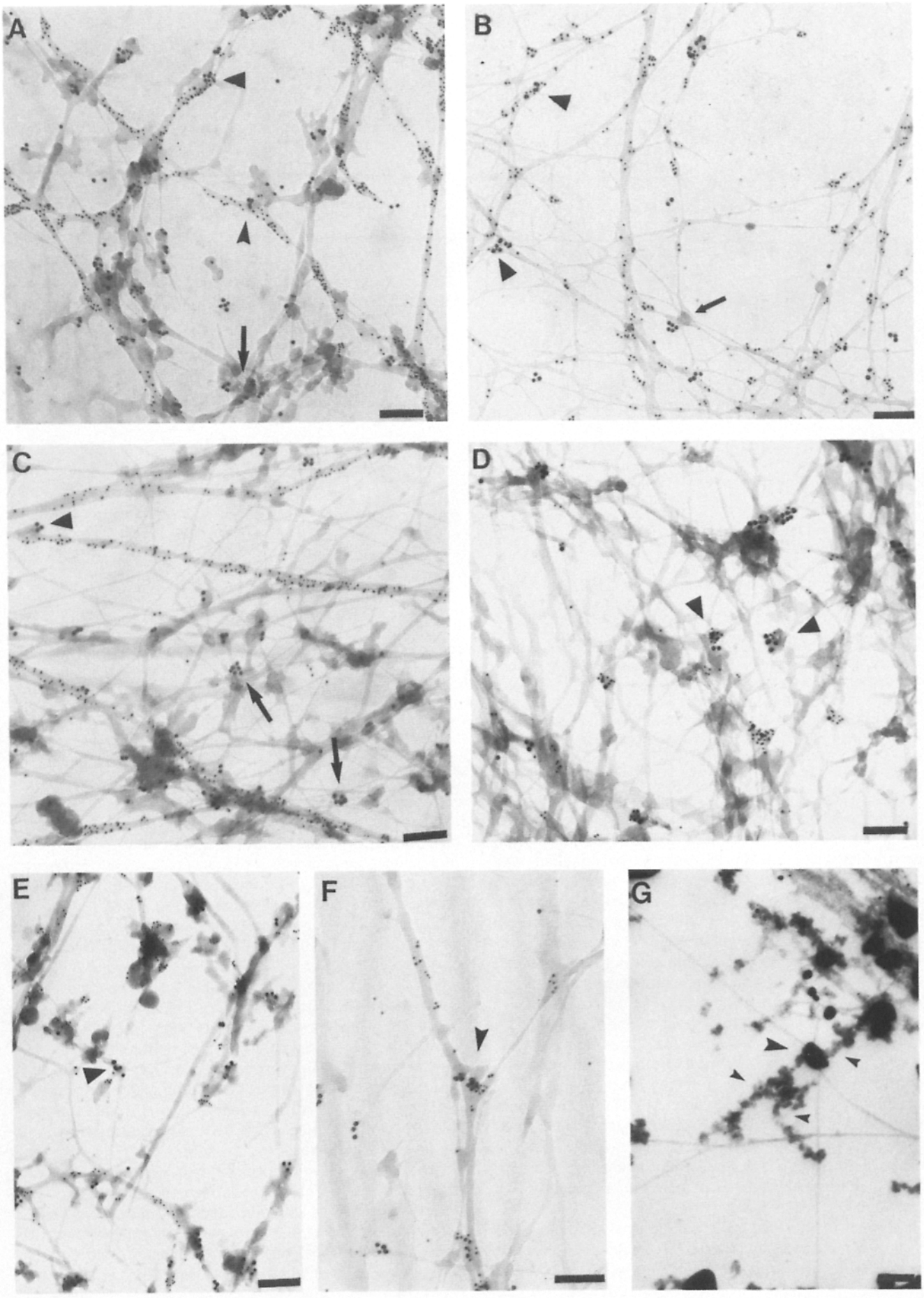
A
B
C
D
E
F
G

Table I. Colocalization of poly(A) mRNA with Cytoskeletal Proteins

Percent of total Poly(A)		
Actin	Vimentin	Tubulin
72.0 ± 10.5	28.9 ± 7.2	*9.8 ± 1.5
Filamin	α-Actinin	EF-1α
44.2 ± 12.1	41.6 ± 6.0	63.1 ± 8.2

Cells were Triton extracted in cytoskeletal buffer at 4°C before fixation (see Materials and Methods). Samples were hybridized with biotinated oligo-dT. The probe and cytoskeletal proteins were detected simultaneously by double label immunogold. The percentage of poly(A) mRNA which localized within 5 nm of labeled proteins is indicated above with standard deviation between three experiments. Five cells were evaluated for each pairwise combination and between three to six micrographs were taken from each cell (magnification 46,000X). This analysis is compiled from over 1,500 oligo-dT signals (~150 micrographs).

* Cells were Triton extracted at room temperature to prevent depolymerization of microtubules.

colocalization of poly(A) mRNA with microfilaments, intersections also appeared to be the site of poly(A) mRNA localization to intermediate filaments (Fig. 5 *B*, *arrowheads*).

The above results were obtained on cells which were Triton extracted at 4°C resulting in microtubule depolymerization. To investigate the possibility that a component of mRNA was localized to microtubules in fibroblasts, Triton extractions were performed at room temperature in the presence of EGTA (Singer et al., 1989). These conditions, although suboptimal for mRNA retention on the other filament systems did allow preservation of many microtubules. The majority of the poly(A) signal was clearly localized to filaments other than microtubules (see Fig. 4 *C*). Less than 10% of poly(A) mRNA colocalized within 5 nm of labeled microtubules. This label however appears to represent bona fide hybridization to poly(A) mRNA, since nonspecific binding of control oligo-dA probes on the labeled microtubules was minimal (signal to noise ratio on the microtubules was 8.3:1).

Since poly(A) predominates at intersections (Fig. 4), composed mainly of actin filaments (Fig. 5 *A*), they would be expected to be in close proximity to actin cross-linking proteins. The localization of poly(A) mRNA with intersections was then further investigated with the above double-labeling method using antibodies to actin cross-linking proteins, ABP50 (EF1α), filamin, and α-actinin. As expected, poly(A) mRNA which localized to points of contact between branched filaments showed strong colocalization with these actin-binding proteins (Fig. 5, *D–F*). Greater than 40% of total detected poly(A) mRNA colocalized within 5 nm of an actin-binding protein signal (Table I). In addition, when the presence of polysomes was analyzed after labeling for these actin-binding proteins, their spatial coincidence was also observed in thin sections (For filamin, see Fig. 5 *G*).

The spatial congruence of mRNA with cytoskeletal filaments has been studied in cells which are Triton extracted before fixation. Because of the possibility that subtle changes in positioning may occur during extraction, it was of interest to determine whether these interactions could be observed in unextracted cells. The distribution of poly(A) mRNA was similar in both Triton-extracted and -unextracted cells which were Epon embedded and thin sectioned (Fig. 2); however, cytoskeletal filaments were not visualized in the unextracted samples. We have recently investigated the application of reagents directly onto thin sections using permeable resins to evaluate mRNA–cytoskeletal colocalization in unextracted cells. An additional advantage of postembedment in situ hybridization is its compatibility with fixed tissue samples. Shown in Fig. 6 *A* is hybridization to poly(A) mRNA in developing muscle which was embedded into Lowicryl and sectioned prior to the hybridization. Cytoskeletal filaments were easily visualized and poly(A) mRNA was spatially overlapping cytoskeletal filaments, in this case, possibly intermediate filaments, but not other organelles (Fig. 6 *A*). Double-label analysis demonstrated that the majority (but not all) poly(A) colocalized with actin protein (Fig. 6 *B*).

Resolution of Single mRNA Molecules

The stoichiometric relationship of the gold detection to the amount of probe hybridized is not known, i.e., how many gold particles correspond to a single poly(A). For instance, dense clusters of gold particles could result from the binding of at least two primary antibodies to a single probe molecule (having multiple biotinated nucleotides), as well as the binding of several secondary antibodies to a primary antibody. Alternatively, these clusters could occur from the colocalization of multiple mRNA molecules. Therefore three levels of amplification could account for a colloidal gold cluster (multiple mRNAs, primary or secondary antibodies). To investigate the stoichiometry of the poly(A) detection, ultrastructural methods to permit the unequivocal identification of a single poly(A) mRNA molecule were developed. This was necessary to determine how individual mRNA molecules are positioned and spaced within the cytoskeleton. The approach used a sensitive colloidal gold detection method which resulted in a stoichiometry of one gold particle for one probe molecule. To couple the detection (a gold particle) with a target mRNA molecule, a single biotin moiety was attached at the 5′ end of the oligo dT probe. The direct detection of these singly labeled probe molecules used an antibody to biotin followed by protein A–labeled gold, an F_c receptor which binds to immunoglobulins at a 1:1 ratio.

Figure 5. Association of poly(A) mRNA with specific cytoskeletal proteins. Double label colloidal gold analysis using whole-mount electron microscopy (critical point drying of Triton-extracted cells which are not resin embedded). Poly(A) is detected with 10-nm gold, and the cytoskeletal protein with 5-nm gold. (*A*) Majority of poly(A) mRNA molecules are associated with microfilaments labeled with antibody to actin. Hybridization is near regions of intersection (*arrowhead*). Some poly(A) mRNAs were not associated with actin (*arrow*). (*B*) Poly(A) mRNA associated with vimentin filaments, near regions of intersection (*arrowheads*). Other poly(A) mRNAs were not associated with vimentin (*arrow*). (*C*) Majority of poly(A) mRNAs (*arrows*) were not associated with microtubules. Some hybridization signal was observed along microtubules. (*arrowhead*). (*D*) Colocalization of poly(A) mRNA with EF1α (*arrowheads*). (*E*) Colocalization of poly(A) mRNA with α-actinin (*arrowhead*). (*F*) Colocalization of poly(A) mRNA with filamin (*ABP 280*). (*G*) Association of polysomes (*small arrowheads*) with an actin vertex, detected by silver enhanced anti-filamin binding (*large arrowhead*) in thin section of Triton-extracted cell. Bar, 100 nm.

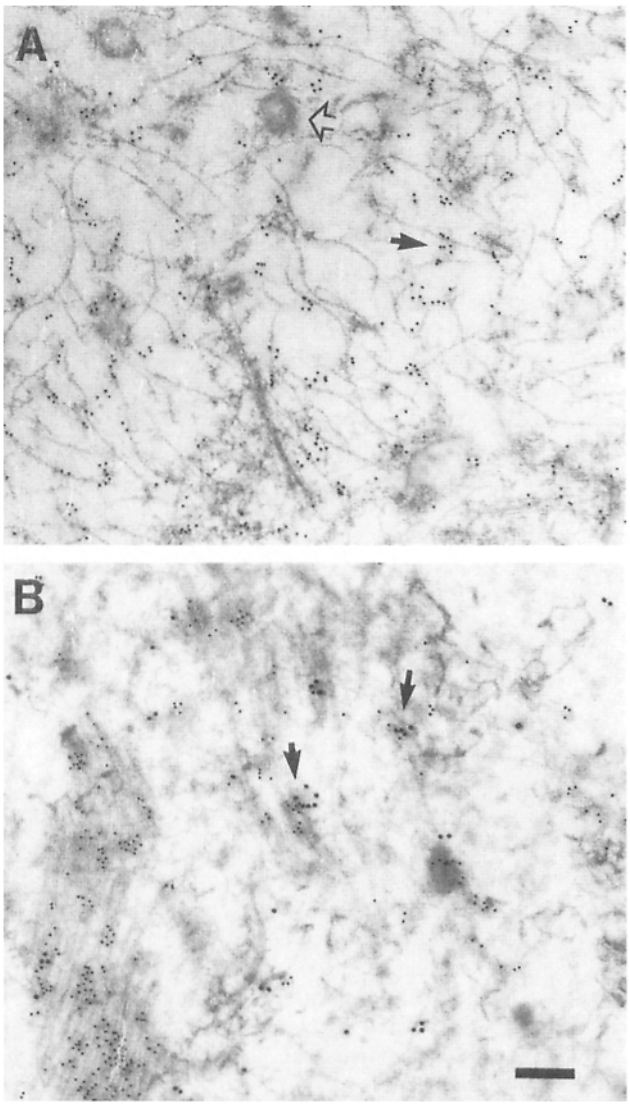

Figure 6. Ultrastructural localization of poly(A) mRNA directly in thin sections. 16-d-old chicken embryo pectoral muscle was fixed and embedded in Lowicryl and sections were exposed to hybridization (see Materials and Methods). (*A*) Hybridization was localized to cytoskeletal filaments (*arrow*). Other cellular structures, i.e., organelles, were not labeled (*open arrow*). (*B*) Double label colocalization of poly(A) mRNA (10 nm) and actin protein (5 nm) (*arrows*). Bar, 200 nm.

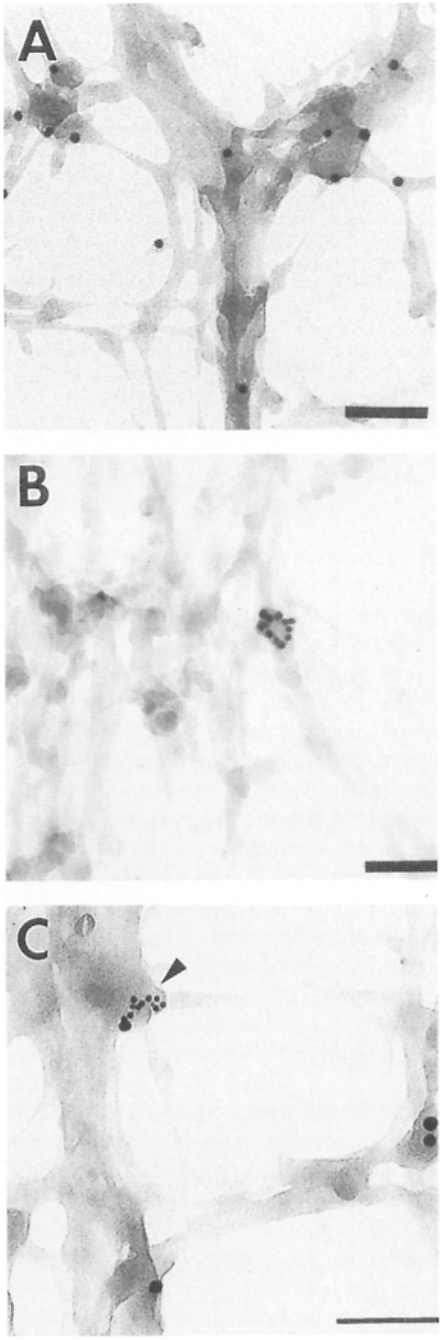

Figure 7. Ultrastructural detection of single poly(A) mRNA molecules. (*A*) Hybridization of oligo-dT with a single 5′ biotin was detected using antibiotin and protein A (10-nm gold) in Triton-extracted and critical point–dried cells. Majority of hybridization signal was observed as single gold particles (91%), which correspond to detection of single oligonucleotide probe molecules. (*B*) Hybridization of unlabeled oligo-dT primer extended in situ using reverse transcriptase in the presence of biotinated dUTP. Cells were washed in 50% formamide 2X SSC after hybridization and transcription. At this stringency, oligo-dT hybrids (not extended by reverse transcriptase) are melted. Detection of biotin labeled cDNA was by antibiotin antibody followed by protein A (10 nm). (*C*) Hybridization of oligo-dT with a single 5′ biotin was extended in situ using reverse transcriptase in the presence of digoxigenin dUTP. Heteroclusters were detected (*arrowhead*) using antibiotin antibody and protein A (10 nm), followed by sheep antidigoxigenin (5 nm). Bar, 100 nm.

The detection of the oligo-dT probe with a single biotin group using protein A (10-nm gold) was initially confirmed by silver enhancement and light microscopy before the ultrastructural analysis (data not shown). The detection of oligo-dT probes containing a single biotin revealed that there was a significant decrease in cluster size: >90% of the hybridization signal was in the form of individual gold particles (Fig. 7 *A*). The number of single gold particles was significantly above background as determined by comparison to the oligo-dA probe control (signal to noise ratio of 9:1). Therefore, the single gold particles must have resulted from the detection of a single biotin and hence a single mRNA. Although no large clusters (less than four particles) were observed with the probe containing a single biotin detected by protein A,

Table II. Ultrastructural Detection of Primers and Reverse Transcripts In Situ

Single 10 nm	Single 10 nm	Multiple 10 nm	Multiple 10 nm
Single 5 nm	Multiple 5 nm	Single 5 nm	Multiple 5 nm
32%	61%	4%	3%

In situ hybridization detected by 10-nm gold was performed with biotin-labeled oligo-dT (chemically modified with a single biotin group) followed by reverse transcription in the presence of digoxigenin-11-dUTP detected by 5-nm gold. See Materials and Methods. The majority of this double label signal (heteroclusters) contained single 10-nm gold particles which corresponded to the detection of an oligo-dT primer molecule, and multiple 5-nm gold particles which corresponded to detection of the synthesized cDNA. Heteroclusters which contained a single 10-nm particle, and multiple 5-nm particles were only rarely observed when control oligo-dA (biotin) primers which were extended with reverse transcriptase (signal to noise rato of 25:1). Analysis was of 100 clusters in three separate experiments.

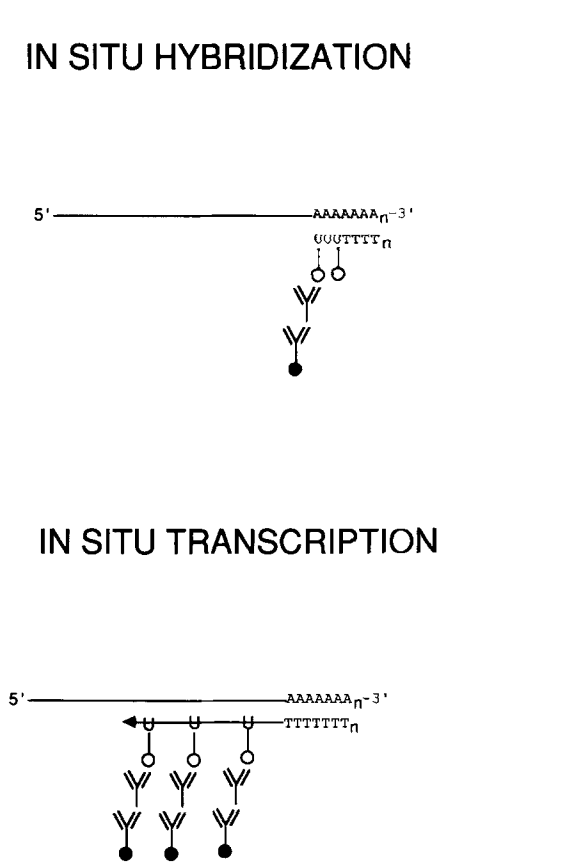

Figure 8. Schematic comparison of in situ hybridization and in situ transcription.

10% of the signal was still in the form of small clusters (two or three particles). These could either represent hybridization of multiple oligo dT probes per poly(A) sequence (50–70 bases; Sheiness et al., 1973), or to multiple poly(A) mRNA molecules. This methodology also confirmed the observation that the majority of scored poly(A) mRNA was localized to cytoskeletal intersections. Messenger RNA molecules were frequently observed in close proximity to one another (within distances of 100 nm, Fig. 7 *A*).

To confirm that a single mRNA had been visualized an additional methodology was developed. The *cis*-poly(A) sequences within the mRNA were used to prime incorporation of biotinated nucleotides using the mRNA as a template and oligo-dT as the primer for reverse transcriptase. Detection was accomplished as above, using protein A such that a single gold particle corresponded to a single biotin moiety. Reverse transcriptase has been used previously in situ to synthesize cDNA using oligo-dT primers, producing a heterogeneous mixture of cDNA lengths (Tecott et al., 1988). In situ transcription methods have recently been reviewed (Eberwine et al., 1993). A comparison of ISH and in situ transcription (IST) with oligo-dT primers is shown in the schematic diagram (Fig. 8). Using in situ hybridization, biotin-labeled oligo-dT probes are hybridized only to the poly(A) sequence of mRNA. Using in situ transcription, the oligo-dT primer is extended using reverse transcriptase in the presence of biotinated nucleotides. Antibody binding is therefore possible at multiple sites along the length of an mRNA and only the transcript is detected. In contrast to the in situ hybridization result yielding a single gold particle per poly(A), clusters of gold particles from a single hybridization event would be expected by IST from the incorporation of multiple biotins.

By light microscopy IST yielded a more significant signal compared to ISH for the same reaction times of silver enhancement (Fig. 9 *A*). The intracellular distribution of the IST signal was indistinguishable from ISH. No specific label was incorporated when oligo dA was used instead of oligo dT (Fig. 9 *B*). At the ultrastructural level, the increase in clusters resulting from the incorporation of multiple biotins was immediately evident; 20% of the signal was observed in groups containing greater than five particles (Fig. 7 *B*). These clusters were in characteristic arrays with relatively constant spacing between particles, and were often in circular or spiral conformations (see also Singer et al., 1989). That the clusters resulted from reverse transcriptase incorporation of the analog nucleotide into a cDNA strand was further confirmed by showing that the IST hybrids have a higher melting temperature than those detected using in situ hybridization. Due to the lower melting temperature of the A-T hybrid, oligo dT probe hybridization is optimal at 15% formamide concentration and a major reduction in signal was observed after a 50% formamide wash following hybridization (Taneja et al., 1992). By contrast, in samples which were reverse transcribed after hybridization, signal was not reduced by washing in 50% formamide after reverse transcription, indicating that increased thermal stability resulted from the synthesis of a contiguous strand (Fig. 7 *B*).

To confirm further that large groups of gold particles were derived from single mRNA molecules, the oligo dT primer and the resulting cDNA were visualized simultaneously. The primer was labeled synthetically on the 5′ end linker arm with biotin and the synthesized cDNA was detected simultaneously by using digoxigenin-labeled nucleotides in the transcription reaction (labeling on the 3′ end prevented priming). The primer was detected as previously described with 10-nm gold and the transcript detected by an antidigoxigenin antibody directly labeled with gold (5-nm). Many primers (35%) and the synthesized cDNA (5-nm particles) were detected together, at the same location. At the ultrastructural level, this signal was observed in the form of dense clusters of gold particles containing both sizes of gold in a reproducible ratio (heteroclusters). The primer was detected by a single gold particle, whereas the synthesized transcript yielded multiple gold particles (Table II). Fig. 7 *C* demonstrates

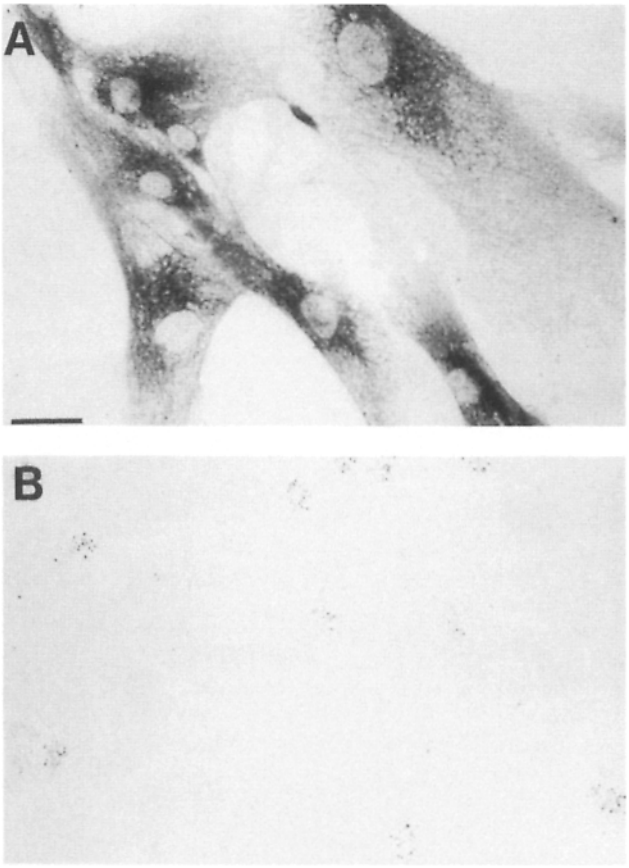

Figure 9. Light microscopic detection of poly(A) mRNA using reverse transcription of oligo-dT primers in situ. (*A*) In situ hybridization with oligo-dT (unlabeled) to Triton-extracted, glutaraldehyde-fixed fibroblasts. Reverse transcriptase catalyzed cDNA synthesis in the presence of biotin-16-dUTP. Detection of antibiotin and protein A (10 nm) was by silver enhancement. Poly(A) mRNA was detected in the cytoplasm, and the distribution was comparable to that observed previously using in situ hybridization with oligo-dT-biotin. Nuclear poly(A) was not detectable with large colloidal gold complexes. (*B*) In situ hybridization with control oligo-dA primer and transcription with biotin-16-dUTP, demonstrating the low background levels obtained with this method. Bar, 20 μm.

bona fide signal: the presence of a single 10-nm particle representing the primer hybridized to the 3′ end of the mRNA followed by several 5-nm gold particles representing the cDNA synthesized from that mRNA template. The double criteria of hybridization as well as priming increased the fidelity of the identification of a single mRNA. A signal to noise ratio of 25:1 (n = 100) (Table II) was obtained from the quantitative analysis of heteroclusters containing both sizes of gold particles when comparing oligo-dT with oligo-dA primers (both probes labeled with a single biotin group). Consistent with previous observations, the majority of the transcripts colocalized with actin (data not shown).

Discussion

We have identified the cytoskeletal filaments which are components of the mechanism controlling the spatial organization of poly(A) mRNA. Unlike previous approaches using indirect means by biochemical fractionation or drug treatments, this work directly visualized mRNA molecules in situ on identified filaments. The fine structure distribution of poly(A) mRNA molecules could be evaluated with a degree of spatial resolution (nanometers) and quantitative accuracy previously not possible. This extensive examination has provided the relative contribution of each of the three filament systems for poly(A) RNA localization in fibroblastic cells, with the approximate stoichiometry of 10:4:1, MF/IF/MT. This is the first time all of the cytoskeletal elements have been implicated in mRNA localization in a single cell type. It confirms and extends previous work using light microscopy which has focussed on microfilaments as an attachment site for poly(A) or actin mRNA (Taneja et al., 1992; Singer et al., 1989; Sundell and Singer, 1991). This work also provides direct evidence for the colocalization of poly(A) mRNA with intermediate filaments. Similarly, GFAP mRNA was observed to colocalize with intermediate filaments in astrocytes using ultrastructural in situ hybridization (Erickson et al., 1992). Using a biochemical approach, veg-1 RNA was found enriched in a cytokeratin fraction in Xenopus oocytes (Pondel and King, 1988).

Microtubules were found to play a minor role in the localization of poly(A) mRNA to the fibroblast cytoskeleton. However, the microscopic evaluation in this work provides only information about the steady state distribution of mRNA. It is possible that mRNAs being actively transported along microtubules would not be a significant component of the current analysis. Transport of veg-1 RNA (Yisraeli et al., 1990) and bicoid RNA (Pokrywka and Stephenson, 1991) was disrupted by microtubule depolymerization. Similarly, myelin basic protein mRNA microinjected into oligodendrocytes formed mobile granuals which localized along microtubules using double label image analysis (Ainger et al., 1993). In some cell types, microtubules appear to play a major role in mRNA localization. For example, the majority of poly(A) mRNA was localized to microtubules in neuronal processes (Bassell et al., 1994). In *Drosophila* embryos, the transport and anchoring of bicoid RNA to the anterior pole could be disrupted by microtubule depolymerization (Pokrywka and Stephenson, 1991). Therefore, mRNA–cytoskeletal interactions may differ between cell types.

The demonstration that a significant amount of poly(A) mRNA is distributed on multiple filaments within a single cell type has several implications. It is currently unknown how different mRNAs can be localized to their appropriate cellular locations. The involvement of multiple filament systems may provide the major component for this sorting. In the simplest model, each filament system could provide binding sites for distinct classes of mRNA. It is likely however that mRNA binding involves additional cytoskeletal proteins besides the core filaments. For example, the poly(A) RNA signal did not decorate either of the filaments but appeared to be associated with vertices. The localization of mRNA to "intersections" suggests that components of the intersection, rather than a direct association with the core filament, are involved in the mechanism of mRNA attachment to the cytoskeleton. Possible candidates for this mechanism are actin binding proteins present at the intersections. The actin binding proteins, filamin (ABP 280), and α-actinin are known to be involved in the assembly of branched microfilament networks (Hartwig and Kwiatkowski, 1991;

Vandekerckhove, 1990). Poly(A) mRNA was frequently colocalized with filamin and/or α-actinin although most intersections containing filamin and α-actinin do not contain poly(A) mRNA. Possibly, these vertices represent unoccupied binding sites for poly(A) mRNA, or alternatively, other unidentified proteins present at these intersections may be specific for poly(A) mRNA binding to the vertex.

The ultrastructural data obtained here indicate that EF1α an actin cross-linker, ABP50, in *Dictyostelium* (Yang et al., 1990) is also present at intersections also containing poly(A) mRNA; therefore, these may be sites of translation of mRNA. The presence of polysomes at these sites provides further support for this interpretation. The association of mRNA with the vertex may therefore be the physical manifestation of translational control. Comparison of in vitro translation efficiencies of mRNAs from soluble and cytoskeletal fractions suggests that mRNA is efficiently translated only when bound to the cytoskeleton (Farmer and Penman, 1981). Additionally, preferential synthesis of viral proteins was achieved by displacing host mRNAs from the cytoskeleton (Lenk and Penman, 1979; Bonneau et al., 1985). Hence, the vertex may be the site where mRNA, ribosomes, and translational factors are sequestered.

Individual mRNA molecules have never before been visualized in situ. Two technological advances permitted this: the use of a chemically modified oligonucleotide probe which contained a single biotin permitted coupling of hybridization and detection stoichiometry and the use of this probe also as a primer to synthesize cDNA, with simultaneous detection. This yielded results consistent with single molecule detection: a single primer detected with one 10-nm gold particle spatially congruent with a cluster of 5-nm gold particles representing the reverse transcript. Because of the spatial colocalization of two independent events, each detection represented a single molecule with high confidence (96% determined by the ratio of events using oligo dA as a control).

The detection of single primers by individual gold particles, as well as detection of the synthesized cDNA by tightly linked series of smaller gold particles was consistent with the majority of the hybridized intersections containing a single mRNA molecule (Table II). A small percentage of the hybridization signal (<10%) could be attributed either to multiple mRNAs per vertex or long poly(A) on a single molecule. Individual mRNAs were frequently observed by gold clustered into circular or spiral conformations rarely in linear arrays. This suggests that the mRNA molecule is not in an extended or linear conformation. Circular mRNAs have also been observed from isolated preparations of mRNA deposited onto grids (Hsu and Coco-Prados, 1979; Ladhoff et al., 1981). Conformations of circular polysomes suggested that the 3′ end of the coding sequence was close enough to reinitiate translation on the same molecule (Christenson et al., 1987). It is possible that interactions between 3′ and 5′ ends of mRNA are also a factor in translational control. Poly(A) sequences have been shown to be required for translation in yeast (Sachs and Davis, 1989) and promote the efficiency of translation in vivo and in cellfree systems (Munroe and Jacobson, 1990).

Messenger RNA–cytoskeletal interactions might be used to synthesize functionally related proteins or multipolypeptide complexes in close proximity. This may be important in the assembly of complex cellular structures such as a sarcomere, or an adhesion plaque. This process could be achieved by the targetting of multiple mRNA molecules to vertices (average 100-nm apart) which are close enough to facilitate interactions of nascent polypeptides. The mRNA–vertex interaction therefore may represent a fundamental binding site where specific proteins are synthesized within "microdomains", perhaps achieving high concentrations in this specific region. This site may represent the "anchoring" component of the mRNA localization mechanism (Singer, 1992), with the vertex as the receptor and poly(A) as the ligand (Taneja et al., 1992). Positioning of specific mRNAs within the cell would then result in a mechanism by which assembly of structural and/or functionally related proteins could be spatially controlled (Kislauskis et al., 1993; Singer, 1993).

We would like to thank Jeanne Lawrence and Susan Billings-Gagliardi for helpful discussions. We thank Christine Dunshee for photographic assistance. We thank Joan Politz for critical review of this manuscript. Antibody to EF1α was kindly provided by Wim Moller (Rijks University, Leiden, The Netherlands).

Supported by National Institutes of Health grant HD18066 to R. Singer. Presented in parts at ASCB annual meetings (1991–1993).

Received for publication 21 February 1994 and in revised form 25 May 1994.

References

Ainger, K., D. Avossa, F. Morgan, S. J. Hill, C. Barry, E. Barbarese, and J. H. Carson. 1993. Transport and localization of exogenous myelin basic protein mRNA microinjected into oligodendrocytes. *J. Cell Biol.* 123: 431–441.

Altman, L. G., B. G. Schneider, and D. S. Papermaster. 1984. Rapid embedding of tissues in Lowicryl K4M for immunoelectron microscopy. *J. Histochem. Cytochem.* 32:1217–1223.

Bassell, G. J. 1993. High resolution distribution of mRNA within the cytoskeleton. *J. Cell Biochem.* 52:127–133.

Bassell, G. J., and R. H. Singer. 1993. Ultrastructural in situ hybridization using immunogold. *In* Electron Microscopy in Viral Diagnosis and Research. M. A. Hyatt and B. T. Eaton, editor. *CRC Press.* 377–411.

Bassell, G. J., R. H. Singer, and K. S. Kosik. 1994. Association of poly(A) mRNA with microtubules in processes of cultured neurons. *Neuron.* 12: 571–582.

Ben-Ze'ev, A., M. Horowitz, H. Skodnik, R. Abulafia, O. Laub, and Y. Aloni. 1981. The metabolism of SV40 RNA is associated with the cytoskeletal framework. *Virology.* 111:475–487.

Bendayan, M. 1983. Ultrastructural localization of actin in muscle, epithelial and secretory cells by applying the protein A-gold immunocytochemical technique. *Histochem. J.* 15:39–58.

Biggiogera, M., S. Fakan, S. H. Kaufmann, A. Black, J. H. Shaper, and H. Busch. 1989. Simultaneous immunoelectron microscopic visualization of protein B23 and C23 distribution in the HeLa cell nucleolus. *J. Histochem. Cytochem.* 37:1371–1374.

Bonneau, A. M., A. Darveau, and N. Sonenberg. 1985. Effect of viral infection on host protein synthesis and mRNA association with the cytoplasmic cytoskeletal structure. *J. Cell Biol.* 100:1209–1218.

Brawerman, G. 1981. The role of the poly(A) sequence in mammalian messenger RNA. *CRC Crit. Rev. Biochem.* 10:1–38.

Carter, K. C., K. L. Taneja, and J. B. Lawrence. 1991. Discrete nuclear domains of poly(A) RNA and their relationship to the functional organization of the nucleus. *J. Cell Biol.* 115:1191–1202.

Cervera, M., G. Dreyfuss, and S. Penman. 1981. Messenger RNA is translated when associated with the cytoskeletal framework in normal and VSV-infected HeLa cells. *Cell.* 23:113–120.

Christensen, A. K., L. E. Kahn, and C. M. Bourne. 1987. Circular polysomes predominate on the rough endoplasmic reticulum of somatotropes and mammotropes in the rat anterior pituitary. *Am. J. Anat.* 178:1–10.

Eberwine, J., C. Spencer, K. Miyashiro, S. Mackler, and R. Finnel. 1993. Complementary DNA synthesis in situ: methods and applications. *Methods Enzymol.* 216:80–101.

Erickson, P. A., S. C. Feinstein, G. P. Lewis, and S. K. Fisher. 1992. Glial fibrillary acidic protein and its mRNA: ultrastructural detection and determination of changes after CNS injury. *J. Structural Biol.* 108:148–161.

Farmer, S. R., A. Ben-Ze'ev, B. J. Benecke, and S. Penman. 1978. Altered translatability of messenger RNA from suspended anchorage-dependent fibroblasts: Reversal upon cell attachment to a surface. *Cell.* 15:627–637.

Fulton, A. B., K. M. Wan, and S. Penman. 1980. The spatial distribution of polyribosomes in 3T3 cells and the associated assembly of proteins into the skeletal framework. *Cell.* 20:849–857.

Hartwig, J. H., and D. J. Kwiatkowski. 1991. Actin-binding proteins. *Curr. Opin. Cell Biol.* 3:87–97.

Hesketh, J. W., and I. F. Pryme. 1991. Interaction of mRNA, polyribosomes and cytoskeleton. *Biochem. J.* 277:1–10.

Hsu, M. T., and M. Coco-Prados. 1979. Electron microscopic evidence for the circular form of RNA in the cytoplasm of eukaryotic cells. *Nature (Lond.).* 280:339–340.

Jeffery, W. R. 1982. Messenger RNA in the cytoskeletal framework: analysis by in situ hybridization. *J. Cell Biol.* 95:1–7.

Kislauskis, E. H., Z. Li, R. H. Singer, and K. L. Taneja. 1993. Isoform-specific 3′-untranslated sequences sort α-cardiac and β-cytoplasmic actin messenger RNAs to different cytoplasmic compartments. *J. Cell Biol.* 123: 165–172.

Ladhoff, A. M., I. Uerlings, and S. Rosenthal. 1981. Electron microscopic evidence of circular molecules in 9-S globin mRNA from rabbit reticulocytes. *Cell Biol. Int. Rep.* 7:101–106.

Lenk, R., and S. Penman. 1979. The cytoskeletal framework and poliovirus metabolism. *Cell.* 16:289–301.

Lenk, R., L. Ransom, Y. Kaufmann, and S. Penman. 1977. A cytoskeletal structure with associated polyribosomes obtained from HeLa cells. *Cell.* 10:67–78.

Munroe, D., and A. Jacobson. 1990. Tales of poly(A): a review. *Gene.* 91: 151–158.

Nakayasu, H., and K. Ueda. 1985*a*. Ultrastructural localization of actin in nuclear matrices from mouse leukemia L5178Y cells. *Cell Struct. & Funct.* 10:305–309.

Nakayasu, H., and K. Ueda. 1985*b*. Association of rapidly-labelled RNAs with actin in nuclear matrix from mouse L5178Y cells. *Exp. Cell Res.* 160:319–330.

Nakayasu, H., and K. Ueda. 1986. Preferential association of acidic actin with nuclei and nuclear matrix from mouse leukemia L5178Y cells. *Exp. Cell Res.* 163:327–336.

Nickerson, J. A., and S. Penman. 1991. BioVision: microscopy in three dimensions. *Semin. Cell Biol.* 2:117–129.

Nielson, P., S. Goelz, and H. Trachsel. 1983. The role of the cytoskeleton in eukaryotic protein synthesis. *Cell Biol. Int. Rep.* 7:245–254.

Ornelles, D. A., E. G. Fey, and S. Penman. 1986. Cytochalasin releases mRNA from the cytoskeletal framework and inhibits protein synthesis. *Mol. Cell. Biol.* 6:1650–1662.

Pokrywka, N. J., and E. C. Stephenson. 1991. Microtubules mediate the localization of bicoid RNA during Drosophila oogenesis. *Development.* 113: 55–66.

Pondel, M. D., and M. L. King. 1988. Localized maternal mRNA related to transforming growth factor B mRNA is concentrated in a cytokeratin-enriched fraction from xenopus oocytes. *Proc. Natl. Acad. Sci. USA.* 85: 7612–7616.

Pudney, J., and R. H. Singer. 1979. Electron microscopic visualization of the filamentous reticulum in whole cultured presumptive chick myoblasts. *Am. J. Anat.* 156:321–336.

Sachs, A. B., and R. W. Davis. 1989. The poly(A) binding protein is required for poly(A) shortening and 60S ribosomal subunit-dependent translation initiation. *Cell.* 58:857–867.

Sanders, J. 1993. The expression and localization of human elongation factor 1. Ph.D. Thesis, Medical School, State University of Leiden, Leiden, The Netherlands. 168 pp.

Scheer, U., H. Hinssen, W. W. Franke, and B. M. Jockusch. 1984. Microinjection of actin-binding proteins and actin antibodies demonstrates involvement of nuclear actin in transcription of lampbrush chromosomes. *Cell.* 39: 111–122.

Sheiness, D., and J. E. Darnell. 1973. Polyadenylic acid segment in the mRNA becomes shorter with age. *Nature (Lond.).* 241:265–268.

Singer, R. H. 1992. The cytoskeleton and mRNA localization. *Curr. Opin. Cell Biol.* 4:15–19.

Singer, R. H. 1993. RNA zipcodes for cytoplasmic addresses. *Curr. Biol.* 3:719–721.

Sundell, C. C., and R. H. Singer. 1991. Requirement of microfilaments in sorting of actin mRNAs. *Science (Wash. DC).* 253:1275–1277.

Singer, R. H., G. L. Langevin, and J. B. Lawrence. 1989. Ultrastructural visualization of cytoskeletal mRNAs and their associated proteins using double-label in situ hybridization. *J. Cell Biol.* 108:2343–2353.

Taneja, K. L., L. M. Lifshitz, F. S. Fay, and R. H. Singer. 1992. Poly(A) RNA codistribution with microfilaments: evaluation by in situ hybridization and quantitative digital imaging microscopy. *J. Cell Biol.* 119:1245–1260.

Tecott, L. H., J. D. Barchas, and J. H. Eberwine. 1988. In situ transcription: Specific synthesis of complementary DNA in fixed tissue sections. *Science (Wash. DC).* 240:1661–1664.

van Venrooij, W. J., P. T. G. Sillekens, C. A. G. van Eekelen, and R. J. Reinders. 1981. On the association of mRNA with the cytoskeleton in uninfected and adenovirus-infected human KB cells. *Exp. Cell Res.* 135:79–91.

Vandekerckhove, J. 1990. Actin-binding proteins. *Curr. Opin. Cell Biol.* 2:41–50.

Visa, N., F. Puvion-Dutilleul, F. Harper, J. P. Bachellerie, and E. Puvion. 1993. Intranuclear distribution of poly(A) RNA determined by electron microscope in situ hybridization. *Exp. Cell Res.* 208:19–34.

Yang, F., M. Demma, V. Warren, S. Dharmawardhane, and J. Condeelis. 1990. Identification of an actin-binding protein from dictyostelium as elongation factor 1a. *Nature (Lond.).* 347:494–496.

Zambetti, G., W. Schmidt, G. Stein, and J. Stein. 1985. Subcellular localization of histone messenger RNAs on cytoskeleton-associated free polysomes in $HeLa_3$ cells. *J. Cell. Physiol.* 125:345–353.